doi: 10.56761/EFRE2022.C4-O-022801

Mixed-mode magnetron and arc deposition of aluminum oxide films

V.O. Oskirko[1,2,], I.M. Goncharenko[1], V.A. Semenov[1], M.I. Azhgikhin[1,2], M.I. Goncharenko[1,3], A.A. Solovyev[1]*

[1]*Institute of High Current Electronics SB RAS, Tomsk, Russia*
[2]*OOO Prikladnaya Elektronika, Tomsk, Russia*
[3]*National Research Tomsk State University, Tomsk, Russia*
[*]*oskirkovo@gmail.com*

Abstract. The paper is devoted to the study of the processes of mixed-mode deposition of aluminum oxide films in oxygen and argon mixture. Mixed-mode is a new pulsed thin film deposition technology that combines magnetron sputtering and arc evaporation. The transition of the magnetron discharge to the arc occurs when the discharge current reaches the threshold value, and the arc burning time is controlled by pulse length. The paper describes the experimental equipment and the principles of controlling the parameters of a combined pulse discharge. The results of measuring the ion current density on a substrate and the deposition rate of aluminum oxide films in mixed-modes at different powers of magnetron and arc discharges are presented. Stable initiation of an arc discharge in a pulsed mode with a "poisoned" cathode surface occurs at a cathode current density of 0.4–0.6 A/cm^2. With the same average discharge power in mixed-mode, a higher average ion current density on a substrate, higher coating deposition rate and more intensity of plasma radiation are provided, compared with medium-frequency magnetron sputtering.
Keywords: Mixed-mode, magnetron sputtering, pulse arc evaporation, aluminum oxide.

1. Introduction

Vacuum arc evaporation and magnetron sputtering are the main methods of physical vapor deposition (PVD) of wear-resistant and other functional coatings on an industrial scale. Vacuum-arc evaporation is the dominant method of tool coating technology [1, 2]. Magnetron sputtering makes it possible to obtain microdroplets-free coatings, but due to the low level of ionization of the sputtered material, in most cases it loses to arc evaporation in terms of the tribological properties. To minimize the disadvantages of both methods, it is advisable to implement hybrid systems in which arc evaporation is combined with magnetron sputtering [3–6]. The goal in this case is to obtain coatings with a minimum number of microdroplets, whose properties are similar to those of coatings obtained by the arc method. In hybrid systems, parallel use of arc evaporators and magnetron sputtering systems is possible. There are also universal sputtering systems that can operate in both modes. In the new mixed-mode technology, the combination of magnetron and arc deposition is realized using a magnetron sputtering system [7]. The arc is ignited on the cathode surface in a pulsed mode when the magnetron discharge current reaches the threshold value, and this causes an increase in the degree of ionization of the sputtered material. The pulsed arc can be initiated at a high repetition rate without the use of arc ignition system. Mainly, mixed-mode is used for graphite target sputtering, which can increase the degree of ionization of sputtered carbon atoms and obtain diamond-like films with high hardness [8, 9]. However, not only graphite can be used as a target material in a mixed-mode. To implement the mixed-mode, one can use the high tendency of aluminum to form arcs during reactive magnetron sputtering. The alpha phase of aluminum oxide (α-alumina) is of practical interest as protective coating, since it has high hardness and temperature stability. To obtain α-alumina, high synthesis temperatures are required. It was shown in [10] that using arc evaporation, with the addition of chromium as a template, it is possible to synthesize the α-alumina films at synthesis temperatures below 600 °C. However, there are problems of poor stability and controllability of the process, which are associated with the continuous nature of the arc evaporators operation at direct current. The pulse nature of the arc in the mixed-mode can

overcome the continuous arc limitations. This paper presents the experiments results of aluminum-target sputtering in an oxygen environment in a mixed-mode mode that combines medium-frequency magnetron sputtering (MFMS) and pulsed arc evaporation (PAE). The electrical parameters of the discharge are investigated and the conditions for stable arc initiation during each pulse are determined. Several modes differing in pulse length and pulse frequency were compared. The deposition rate, ion current density on a substrate, plasma radiation intensity and hardness of coatings obtained at room temperature are compared.

2. Experimental setup

The scheme of an experimental setup for depositing coatings in a mixed-mode is shown in Fig.1. The setup includes a vacuum chamber with pumping and work gas supply systems. Magnetron sputtering system (MSS) with a 100 mm dameter Al target has an unbalanced magnetic field configuration. The magnitude of the magnetic field on the cathode surface in the race track region is 730 G. A high-power pulse power supply (HPPS) and a power supply for medium frequency pulsed magnetron sputtering (MFPS) were used for the experiments.

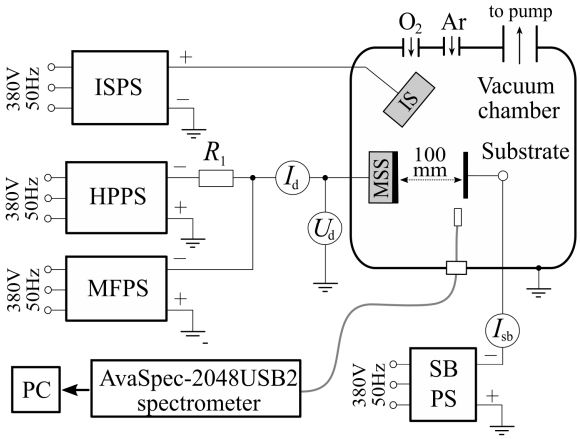

Fig.1. The experimental setup scheme for film deposition in mixed-mode and by magnetron sputtering.

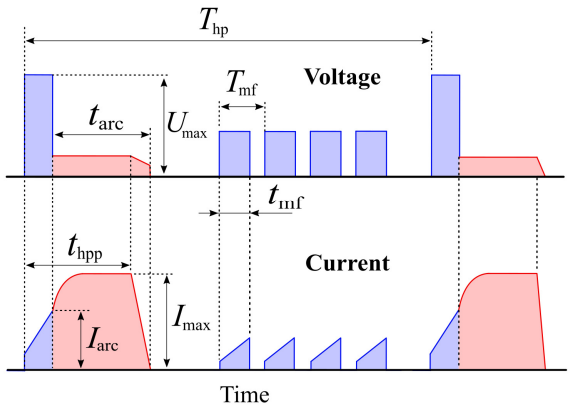

Fig.2. A plot of discharge voltage and current pulses in mixed-mode.

The maximum pulse current at the HPPS output can reach 1 kA, the voltage is 1 kV, the pulse length is 5–250 µs, and the pulse frequency is 20–5000 Hz. The HPPS output has a ballast resistor $R_1 \simeq 1$ Ohm to limit and stabilize the arc discharge current pulse amplitude. MFPS generates current pulses with amplitude up to 15 A, voltage up to 650 V, frequency 1–100 kHz and duty cycle 10–80 %. HPPS and MFPS are connected in parallel and can operate together or separately.

A plot of voltage and current pulses in mixed-mode is shown in Fig.2. Arc powering pulses are generated with a period of T_{hpp}, which includes a high-power pulse with a length of t_{hpp}. During the pause, MFMS pulses are generated. The length t_{hpp} includes the durations of the magnetron and arc discharges. During the magnetron discharge, voltage U_{max} is applied to the discharge gap. Arc initiation occurs when the current increases to the threshold value I_{arc}. After the arc is formed, the load resistance decreases. Most of the voltage U_{max} is applied to the resistor R_1, which limits the discharge current to I_{max}. Until the end of the pulse, the arc burning voltage $U_{arc.}$ is present on the load.

An ion source (IS) equipped with a high voltage power supply (ISPS) was used to clean the substrates before coating. A rotating substrate holder with an area of 70 cm^2 was located at a distance of 70 mm from the target. During the coating process, a constant bias voltage of -100 V was applied to it from the power supply SBPS. Using the sensors and an oscilloscope the discharge

current I_d, the discharge voltage U_d and the ion current to a substrate I_{sb} were measured. Coatings were deposited on substrates made of glass, silicon, and structural steel 40X. The film thickness was measured using an MII-4 microinterferometer (LOMO, Russia). Plasma radiation of the arc discharge was registered by a spectrometer AvaSpec-2048USB2 (Avantes B.V., Netherlands). The optical sensor was located at a distance of 70 mm from the cathode parallel to its surface, as shown in Fig.1.

Substrates made of 40X steel had the shape of a disk 25 mm in diameter and 9 mm high. The initial structural-phase state of the substrate material is ferrite-pearlite. The microhardness of the substrate surface is ~2.8 GPa. The substrates surfaces were mechanically ground and polished to a roughness of Ra ~ 0.02 μm and then thoroughly degreased in the ultrasonic bath.

The film thickness was estimated by two methods: Calotest (Calotest CAT-S-0000, CSEM, Switzerland) and microinterferometry (MII-4, Lomo, Russia). The coating thickness values were used to calculate the deposition rate for each of the modes. Hardness measurements were also carried out by two methods. Nanohardness (H) and elastic modulus (E – Young's modulus) of the surface layers were measured with a CSM Instruments (UK) Nano-Hardness Tester at a load of 10 mN. The penetration depth of the indenter did not exceed 0.2 μm. The results of nanoindentation were processed according to the Oliver-Pharr method [11]. The elastic recovery value of the surface was calculated from the loading-unloading curves using the formula: $W_e = (h_m\text{-}h_f)/h_m$, where h_m – maximum penetration depth, h_f – penetration depth after unloading. Microhardness was measured on a PMT-3 instrument, under a load of 0.4 N. Knoop's diamond pyramid with a rhombic base was used as indenter [12]. The Knoop hardness test method also referred as a microhardness test method is usually used when the samples have thin and brittle coatings, as in our case. The indentations have the form of a strongly elongated rhombus, the large diagonal L is 7 times greater than the small d, the imprint depth h is 30 times less than the length of the larger diagonal. For each sample 5 measurements of microhardness were performed, and then the obtained values were averaged.

3. Results and discussion

Film deposition was carried out in 4 mixed-modes (mode *1–4*) and in one medium-frequency magnetron sputtering mode, in which there was no arcing (mode *5*). Modes *1–4* differed in the length and frequency of the arc powering pulses t_{hpp}. The length t_{hpp} varied from 25 to 200 μs, and the period T_{hpp} varied from 1.5 to 50 μs. The average output power of HPPS was constant at 1.2 kW. For a stable discharge in the pauses between pulses in modes *1–3*, it was necessary to maintain a medium-frequency discharge of low power of 100 W at T_{mf} = 15 μs and t_{mf} = 7 μs. The magnetron discharge power in mode 5 was 500 W at T_{mf} = 15 μs and t_{mf} = 7 μs (Table 1).

Fig.3 presents oscillograms of arc powering pulses in modes *1–4*. The arcing occurs 5–10 μs after the start of the voltage pulse. On Fig. 3e-f on a larger scale shows the oscillograms of voltage, current and power at the moment of transition of the magnetron discharge to the arc. It can be seen that the arc initiation current I_{arc} is 10–35 A, depending on the mode.

Table 1. Parameters of deposition modes

	t_{hpp}, μs	f, Hz	Average output power of HPPS, W	U, V	Average arc current, A	Average arc power, W	Average output power of MFMS, W
Mode 1	200	20	1200	610	2.0	95	100
Mode 2	100	50		600	2.0	132	100
Mode 3	50	150		660	1.8	250	100
Mode 4	25	720		680	1.8	164	0
Mode 5	-	-		-	-	-	500

The arc formation is accompanied by a sharp drop in voltage up to 100–150 V. The high arcing voltage is explained by the presence of a magnetic field on the target surface, which hinders the movement of electrons to the anode. After the arc formation, the rate of growth of the discharge current sharply increases to approximately 50 A/μs, and then gradually decreases. In approximately 30 μs, the discharge current reaches its maximum value $I_{max} \approx 500$ A and retains it until the end of the pulse. The duration of the transient process at the beginning of the arc current pulse is determined by the inductance of the discharge power supply circuit and the resistance R_1.

The transient process in mode *4* does not have time to end due to the short pulse length t_{hpp}, so the current pulse has a smaller amplitude and a triangular shape. From Fig.3g it can be seen that the discharge instantaneous power first sharply decreases after arc the formation, and then increases. For a long arc pulses length (modes *1* and *2*), a sharp decrease discharge power from 40 to 20 kW is observed 60–70 μs after the pulse start. The discharge power decrease is due to a drop in the arcing voltage, which may be associated with a change in the cathode spot location or a change in its type. Perhaps the cathode spot (or several ones) leaves the area with a strong magnetic field, which prevents the movement of electrons to the anode.

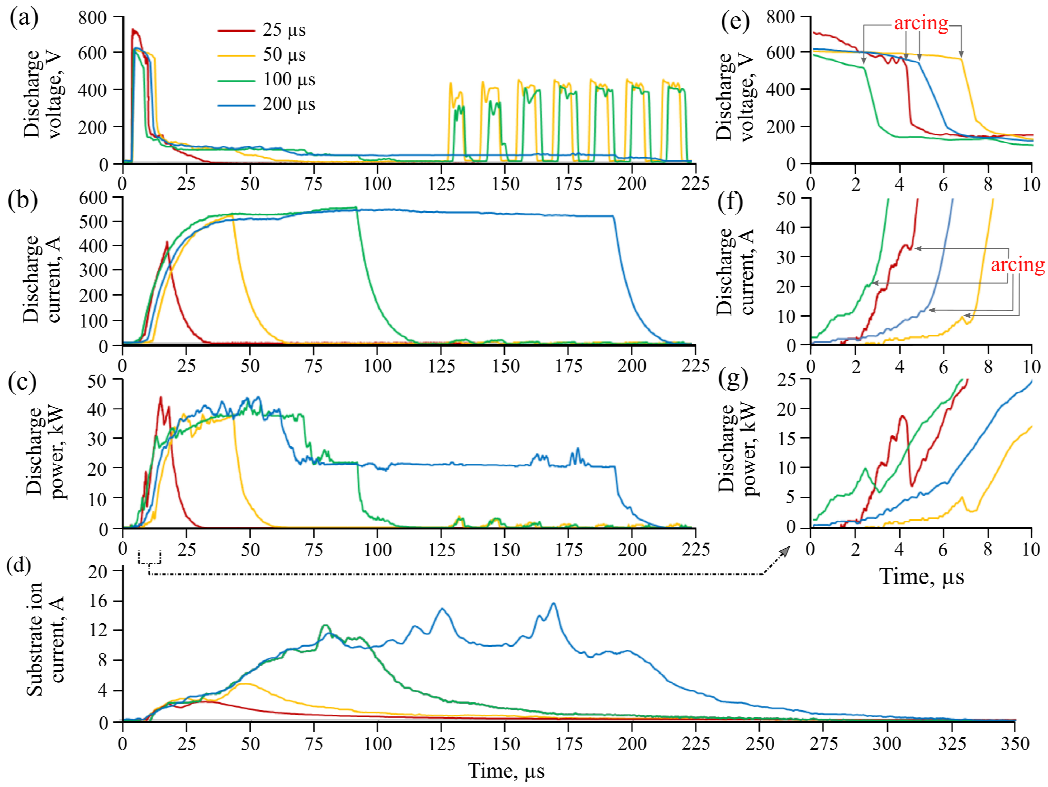

Fig.3. Oscillograms of voltage pulses (a,e), current (b,f) and discharge power (c,g), and also substrate ion current (d) in mixed-modes (modes *1–4*).

In Fig.3d shows the substrate ion current pulse. It can be seen that the length of the arc current pulse has a significant effect on the substrate ion current amplitude. The substrate ion current in mode *4* reaches 3 A, while in mode *2* this value is 12 A. In mode *1*, the ion current growth reaches saturation (12 A) 75 μs after the pulse start. Then, several peaks with amplitude of up to 16 A and a period of approximately 50 μs are observed. After the end of the discharge current pulse, a slow decrease in the substrate ion current is observed for about 100 μs. Table 2 shows the results of measurements of the average ion current density on a substrate j_i and the deposition rate v_d in mode *1–5*.

Table 2. Deposition rate and the ion current density on a substrate

	t_{hpp}, μs	Average discharge power, W	v_d, nm/min	Specific deposition rate, nm/kW*min	I_i, mA	j_i, mA/cm^2	Specific ion current, mA/cm^2*kW
Mode 1	200	195	12.5	64.1	43	0.61	3.15
Mode 2	100	232	9.2	39.5	44	0.63	2.71
Mode 3	50	350	10.7	30.5	46	0.66	1.88
Mode 4	25	164	5.5	33.8	62	0.89	5.40
Mode 5	MF	500	14.7	29.3	23	0.33	0.66

Despite the fact that mode *4* provides the lowest substrate ion current amplitude its integral value is the highest. This is achieved due to the high pulse repetition rate. The average ion current density on a substrate in mode *4* is about 30 % higher than in modes *1–3*.

All mixed-modes (*1–4*) provided a higher ion current density on a substrate compared to the magnetron sputtering mode (mode *5*), despite the lower average discharge power. The highest deposition rate was achieved in mode *5*. This is due to the higher average discharge power in this mode. In terms of specific deposition rate, defined as nm/kW·min, mode *5* provides the lowest productivity. In mixed-modes (mode *1–4*), there is a tendency to increase the deposition rate with an increase in the arc pulses length.

Fig.4 shows the results of optical emission spectroscopy of the plasma in the substrate location. It can be seen that the existence of an arc in mixed-modes significantly increases the radiation intensity of both gas ions and aluminum ions. The intensity of the emission lines increases with an increase in the arc pulses length.

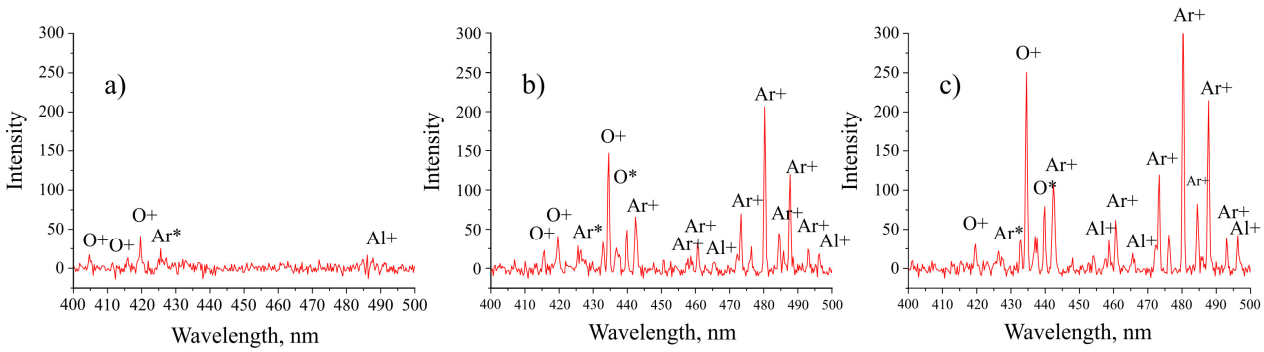

Fig.4. Plasma emission spectra in mode *5* (a), mode *4* (b) and mode *1*(c).

Fig.5 shows photos of the thin film surface deposited in mode *4*. A large number of microdroplets are observed in the film, despite the relatively short arc pulses length (25 μs). The resulting film is non-conductive, which indirectly indicates the content of aluminum oxide in it.

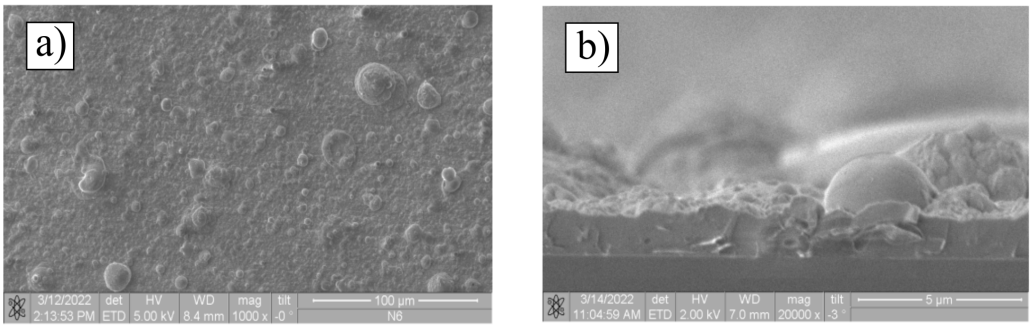

Fig.5. Photos of the coating surface. (a) – top view; (b) – side view. The duration of the process (mode *4*) is 6 hours.

For all modes (see Table 3), there is a tendency to increase in hardness by ~2–3 times compared to the uncoated steel samples (H ~ 2.8 GPa). It should be noted that the microhardness of the coatings is higher than their nanohardness. Obviously, the real properties of the coatings differ from the values obtained experimentally and depend on the measurement methods. Good agreement between the hardness values (~7.0 GPa) measured by both methods is observed for mode *5*.

Table 3. Coating parameters

	Thickness, nm	Nanohardness (H), GPa	Young's modulus, (E), GPA	Micro-hardness, KHN0,4, GPA
Mode 1	1505	5.3±1.0	125.2±17.7	7.33±0/3
Mode 2	1100	6.4±1.3	128.5±25.5	7.63±0.3
Mode 3	1280	4.3±0.1	108.0±2.7	7.21±0.3
Mode 4	1730	3.8±0.4	111.3±7.7	14.02±0.3
Mode 5	1760	7.0±0.1	96.6±0.8	6.59±0.3

However, for mode *4* the measured microhardness value is ~3.5 times higher than the nanohardness value, despite the fact that in both deposition modes (*5* and *4*) the thickness of the films is approximately the same (~1750 nm).

It is known that when indentation of materials with a large ratio of elastic work (more than 20 %) is carried out, the determination of hardness from the recovered indent (microhardness) gives distorted values. Due to the decrease in the indentation diagonal after the removal of the load, compared with the dimensions of the indenter itself, the hardness value will be greatly overestimated. The Young's modulus values for films deposited in mode *4* are significantly higher (111.3 ± 7.7) GPa than for films deposited in mode *5* (96.6 ± 0.8) GPa and therefore the indentation shape will be more distorted. As a result, the microhardness values for mode *4* will be overestimated. These considerations are also valid for coatings deposited in modes *1–3*, but it should be taken into account that these films have a smaller thickness compared to the ones considered above.

The measured hardness values of steel substrates with film deposited in mixed mode are significantly lower than the alumina tabular values (~13.0 GPa). This is probably due to the fact that not a homogeneous film, but a composite one was obtained, which consists of aluminum microdroplets immured in aluminum oxide. The low hardness of the film obtained in mode *5* is due to the low substrate temperature during deposition.

4. Conclusion

The paper demonstrates the possibility of obtaining aluminum oxide films in mixed-mode, which is a combination of medium-frequency pulsed magnetron sputtering and pulsed arc. The arc initiation on the magnetron cathode surface is carried out during each pulse, at the moment when the cathode current density reaches the threshold value. It is shown that the average ion current density on a substrate increases with a decrease in the pulse length and an increase in pulse frequency. This is accompanied by a decrease in the specific deposition rate of the coating. Optical emission spectroscopy showed a significant increase of the emission lines intensity of oxygen, argon, and aluminum ions in the mixed-mode compared to MF sputtering. However, the result of the pulsed arc is a large number of microdroplets in the resulting films. The film hardness ~(4.0–7.0) GPa is noticeably higher than the steel substrate hardness (~2.8 GPa) and aluminum hardness (~0.8 GPa). It is obvious that the change in the mechanical characteristics of the aluminum oxide film is primarily related to its thickness and the deposition modes.

Acknowledgements

The authors acknowledge the financial support from the Russian Science Foundation (Project No. 22-29-00627).

5. References

[1]. Erkens G., Vetter J., Mueller J., Mohnfeld A., *Plasma-Assisted Surface Coating*. (Landsberg: Verlag Moderne Industrie, 2011).
[2]. Boxman R.L., Martin P.L., Sanders D.M., *Handbook of Vacuum Arc Science and Technology*. (New Jersey: Noyes Publications, 1995).
[3]. Buske M.J., Randhawa H.S., *Physical vapour deposition dual coating process*, patent US000005234561A, 1993.
[4]. Vettera J., Kubota K., Isaka M., Mueller J., Krienke T., Rudigier H., *J. Surf. Coat. Technol.*, **350**, 154, 2018; doi: 10.1016/j.surfcoat.2018.05.075
[5]. Munz W.D., Hauzer F.J.M., Schulze D., Buil B., *J. Surf. Coat. Technol.*, **49**, 161, 1991. doi: 10.1016/0257-8972(91)90049-3
[6]. Lee C.S., Lee K.R., Suh S.H., *Mater. Sci. Technol.,* **20**, 1, 2004; doi: 10.1179/026708304225019777
[7]. Lattemann M., Moafi A., Bilek M.M.M., McCulloch D.G., McKenzie D.R., *Carbon*, **48**(3), 918, 2010; doi: 10.1016/j.carbon.2009.10.029
[8]. Tucker M.D., Ganesan R., McCulloch D.G., Partridge J.G., Stueber M., Ulrich S., Bilek M., McKenzie D.R., Marks N.A., *J. Appl. Phys.*, **119**, 155303, 2016; doi: 10.1063/1.4946841
[9]. Akhavan B., Ganesan R., Stueber M., Ulrich S., McKenzie D.R., Bilek M.M., *Thin Solid Films*, **688**, 137353, 2019; doi: 10.1016/j.tsf.2019.06.003
[10]. Ramm J., Ante M., Bachmann T., Widrig B., Brändle H., Döbeli M., *Surf. Coat. Technol.*, **202**, 876, 2007; doi: 10.1016/j.surfcoat.2007.05.044
[11]. Oliver W.C., Pharr G.M., *J. Mater. Res.*, **7**(6), 1564; doi: 10.1557/JMR.1992.1564
[12]. Riester L., Bell T.J., Fischer-Cripps A.C., *J. Mater. Res.*, **16**, 1660, 2001; doi: 10.1557/JMR.2001.0230